processes

MDPI

Article

A Glycopeptide from *Agaricus balchaschensis* Mitigates Cadmium Damage in Mice

Nuerziya Yalimaimaiti [1,†], Yongqiang Dong [2,†], Peisong Jia [1], Xiaobin Feng [3,4,*], Ying Luo [1], Jingzhe Hao [1,*], Wenjie Jia [1], Haoyu Chen [1], Qi Zhu [1], Zhihao Liang [1] and Cheng Luo [1]

[1] Laboratory of Integrated Pest Management on Crops in Northwestern Oasis, Ministry of Agriculture and Rural Affairs, Xinjiang Key Laboratory of Agricultural Biosafety, Institute of Plant Protection, Xinjiang Academy of Agricultural Sciences, Urumqi 830091, China; nrzy@xaas.ac.cn (N.Y.); jiapeisong@xaas.ac.cn (P.J.); sysly@xaas.ac.cn (Y.L.); jwj202407@163.com (W.J.); chenhaoyu@xaas.ac.cn (H.C.); zhuqi@xaas.ac.cn (Q.Z.); lzh033430@163.com (Z.L.); 15276855351@163.com (C.L.)
[2] Laboratory of Medicinal and Edible Fungi, Department of Vegetables, College of Horticulture, China Agricultural University, Beijing 100193, China; yongqiangdong@keymedbio.com
[3] Cang Zhou Academy of Agriculture and Forestry Sciences, Cangzhou 061000, China
[4] Institute of Food Science Technology Nutrition and Health (Cangzhou), Chinese Acedmy of Agriculture Sciences, Cangzhou 061000, China
* Correspondence: fengxiaobin@126.com (X.F.); urmqhjz@xaas.ac.cn (J.H.)
† These authors contributed equally to this work.

Abstract: This study was aimed at extracting, characterizing, and exploring the detoxification activity of the peptide-containing polysaccharide from *Agaricus balchaschensis*. An anion adsorption fraction was acquired through hot water extraction. Its structure was analyzed, and the potential protective effect against cadmium-intoxicated mice was explored. Structural analysis revealed that the principal component of the peptide-containing polysaccharide of *A. balchaschensis* (ABPCP) is polysaccharide, which consists of glucose, mannose, galactose, and xylose, containing (1 → 4)-linked α-D-glucan, (1 → 3)-linked β-D-Glcp, (1 → 4)-linked β-D-Glcp, (1 → 6)-linked β-D-Glcp, (1 → 6)-linked β-D-Manp, (1 → 3)-linked β-D-Galp, (1 → 6)-linked β-D-Galp, and (1 → 4)-linked β-D-xylan. The amino acid content of ABPCP is 11.747 mg/g. Threonine, serine, glutamate, glycine, alanine, cysteine, valine, methionine, lysine, and arginine were detected in ABPCP, among which the content of glutamate was the highest. The alleviating effect of ABPCP on cadmium poisoning in mice was investigated. ABPCP significantly reduced the cadmium content in serum and the heart, kidneys, and liver, which indicates that ABPCP could promote cadmium discharge. ABPCP also significantly decreased serum nitric oxide, endothelin-1, urea, uric acid, and serum creatinine, alleviating kidney and liver damage caused by cadmium. All these results manifest that ABPCP can lower the cadmium content in organs and alleviate the damage to kidneys and livers damaged by Cd.

Keywords: *Agaricus balchaschensis*; peptide-containing polysaccharide; structure

check for updates

Received: 9 December 2024
Revised: 29 December 2024
Accepted: 7 January 2025
Published: 9 January 2025

Citation: Yalimaimaiti, N.; Dong, Y.; Jia, P.; Feng, X.; Luo, Y.; Hao, J.; Jia, W.; Chen, H.; Zhu, Q.; Liang, Z.; et al. A Glycopeptide from *Agaricus balchaschensis* Mitigates Cadmium Damage in Mice. *Processes* **2025**, *13*, 168. https://doi.org/10.3390/pr13010168

Copyright: © 2025 by the authors. Licensee MDPI, Basel, Switzerland. This article is an open access article distributed under the terms and conditions of the Creative Commons Attribution (CC BY) license (https://creativecommons.org/licenses/by/4.0/).

1. Introduction

Natural polysaccharides have attracted a large amount of interest for their biological activity and minimal side effects. Polysaccharides are complex macromolecules that are composed of more than ten monosaccharides connected to each other, including cellulose, hemicellulose, and pectin [1]. There is more and more evidence that polysaccharides exert hypoglycemic, antioxidant, and anti-inflammatory activities [2]. The bioactivity of polysaccharides is correlated with their structures, involving monosaccharide types, the mode of

glycosidic linkage, molecular sizes, tertiary structures, anomeric carbon configuration, and the degree of polymerization [3]; therefore, revealing the structures of polysaccharides is significant when researching them. Peptides hold significant potential for treating various human diseases, including antitumor, anti-diabetic, antimicrobial, and antiviral applications. Compared to secondary metabolites, peptides offer several advantages: they can be chemically modified to enhance stability, are easily synthesized, and provide an environmentally friendly and efficient system for large-scale production. These characteristics make peptides a promising tool for developing alternative therapeutics [4,5].

Nowadays, more and more evidence has revealed that polysaccharides connecting with peptides can also exhibit various activities like polysaccharides, including antioxidant and immunomodulatory activity, acetylcholinesterase inhibition, intestinal flora regulating, and ameliorating renal dysfunction [6–11]. New sources of bioactive polysaccharides from nature are being explored, and at the same time polysaccharide modification and other polysaccharide derivatives are being employed and developed [6,8]. Therefore, exploring new novel polysaccharides and polysaccharide–peptide complexes could provide new insight into their utilization.

Cd has been considered a main heavy metal threat to our health because it can cause severe detrimental effects in different physiological systems involving oxidative stress [12,13]. Exposure to cadmium can lead to uric acid, urea nitrogen, nitric oxide, and creatinine increases in serum [14,15], and can also induce primarily liver damage, whereas chronic exposure is manifested mainly as renal disease [13,16]. Several studies have been conducted to find drugs to reduce the toxicity of Cd. Grape seed procyanidin resisted oxidative damage to kidneys induced by Cd [17], and *Lycium barbarum* polysaccharides also reduced oxidative stress in the liver [18]. Curcumin improved episodic memory in cadmium-induced memory impairment [19]. Many mushrooms are traditional Chinese medicinal materials, and mushroom polysaccharides have been proven to have a variety of biological activities. However, there have been few reports on mushroom substances that reduce cadmium damage [20,21].

Mushrooms contain a variety of bioactive substances, including polyphenols, polysaccharides, peptides, and so on [22]. Polysaccharides have been a research hotspot in recent years. Polysaccharides exist in many mushrooms as polysaccharide–peptides (PSPs) and polysaccharide–triterpenoids [23,24]. There is much evidence indicating that polysaccharide–peptides extracted from mushrooms exhibit various bioactivity. Still, there is little research about *A. balchaschensis* polysaccharide–peptide conjugate [6,7,9,10]. *A. balchaschensis* is a unique edible mushroom in Xinjiang Province, China. It tastes delicious and has high medicinal value. Although it is known to have antioxidant, anti-tumor, and anti-aging properties, there are few relevant studies about it. In this study, peptide-containing polysaccharide was extracted from *Agaricus balchaschensis*. Its structure was analyzed, and its ability to mitigate damage in Cd-induced damaged mice was assessed.

2. Materials and Methods

2.1. Materials and Chemicals

The fruiting bodies of *Agaricus balchaschensis* were collected from Xinjiang Province (China). Ion exchange resins CM-Sepharose and DEAE-Sepharose were from General Electric Co. (Boston, MA, USA). Reagents required for mouse experiments were cadmium chloride solution (Shanghai Maclin Biochemical Technology Co., Ltd. Shanghai, China) concentration 200 μL/mL and physiological saline 2 mL/d; the Olympus CX21 optical microscope, manufactured in Japan (Tokyo, Japan), was utilized for the examination of pathological tissue sections and the performance of cell quantification. All other reagents were of analytical grade and the water used was glass distilled.

2.2. Preparation of Polysaccharide

The first step was the extraction of crude polysaccharides by previously described methods (Figure 1) [25]. Briefly, the powder of the fruiting body was dispersed in water at a ratio of 1:15 (*w*/*v*), and the mixture was heated for 4 h at 95 °C. The extracting solution was collected and mixed with 3 V ethanol. The mixture was kept for 10 h at 4 °C. Precipitates were collected and dissolved in deionized water to deproteinize with the Sevage method. The upper fraction was collected and dialyzed thoroughly against a phosphate buffer (0.05 M, pH 7.4) at 4 °C. The dialyzed solution was subjected to DEAE-Sepharose chromatography and eluted with different solutions (phosphate buffer, 0.15 M NaCl, 0.5 M NaCl, and 1 M NaCl). The fraction eluted by 0.5 M NaCl was collected because it had the highest content. The fraction was then dialyzed against acetate buffer (0.05 M, pH 4.6) at 4 °C, subjected to CM-Sepharose chromatography, and eluted with acetate buffer, and the unbound fraction collected for further analysis was the *Agaricus balchaschensis* peptide-containing polysaccharide (ABPCP) (Figure 2).



Figure 1. Fruit body of *Agaricus balchaschensis*.

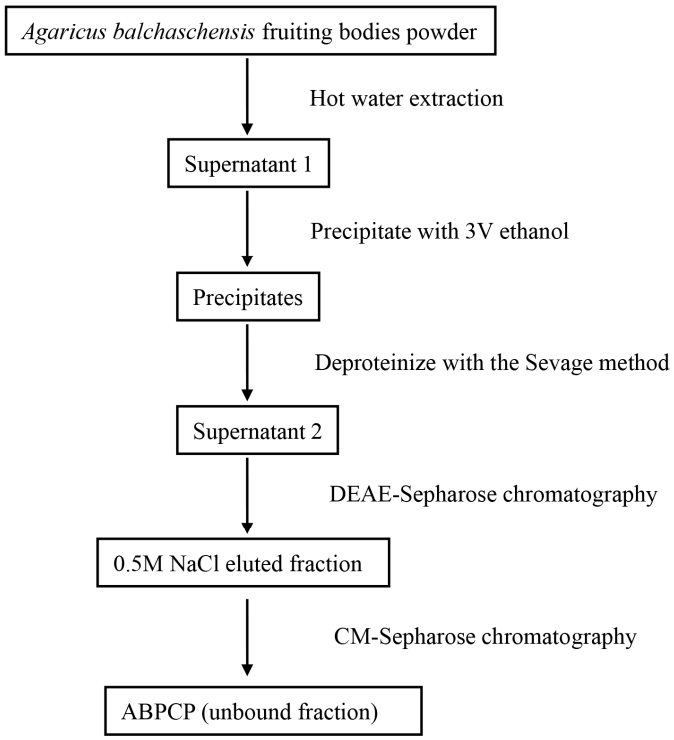


Figure 2. Purification of *Agaricus balchaschensis* polysaccharide (ABPCP) (schematic).

2.3. FTIR and NMR Analysis

The Fourier transform infrared (FTIR) spectrum was recorded on an FTIR spectrometer (Alpha, Bruker, Karlsruhe, Germany) using KBr disks containing 1% finely ground samples. Solution-state ^{1}H, ^{13}C, and heteronuclear single quantum coherence (HSQC) NMR spectra were acquired at 298 K with an Avance III HD 500 spectrometer (Bruker) from samples dissolved in D_2O [26].

2.4. Thermogravimetric Analysis

Thermogravimetric analysis (TGA) and derivative thermogravimetry (DTG) were performed using a simultaneous thermal analyzer (model STA 2500, Netzsch, Free State of Bavaria, Germany). ABPCP powder (~6 mg) was placed in a platinum crucible in an N_2 atmosphere and analyzed in a temperature range of 25–800 °C with a heating rate of 5 °C/min [27].

2.5. Amino Acid Analysis

The CD spectrum was recorded with a J-815 spectropolarimeter (Jasco, Tokyo, Japan) from wavelengths of 250 to 190 nm, with a scan rate of 50 nm/min according to a previously described method [28]. The sample was hydrolyzed with 6 M HCl for 24 h at 110 °C in vacuo [29] and analyzed by an amino acid analyzer (Biochrom 30+, Cambridge, UK).

2.6. Reduction of the Toxicity of Heavy Metals In Vivo

2.6.1. Animal Experiments

Female Kunming strain mice (20 ± 2 g) purchased from the School of Animal Science, Xinjiang Medical University, were acclimated to new conditions for seven days with free access to food and water ad libitum at a temperature of 20–25 °C under a 12 h light/dark cycle. Experiments were performed in accordance with the regulations of the Institutional Animal Care and Use Committees (Issue No: IACUC/20210507/04).

All mice were randomly distributed into three dose groups and two control groups (five mice in each group). Three dose groups and the negative control group had free access to drinking water with 200 μg/mL $CdCl_2$ and were given different concentrations of ABPCP solution. The treatment of experimental groups (intragastric administration for 21 days) was as follows:

Group CK: vehicle control, normal saline.
Group NG: negative control group, normal saline.
Group DG-25: 25 mg/kg ABPCP.
Group DG-50: 50 mg/kg ABPCP.
Group DG-100: 100 mg/kg ABPCP.

At the end of the experiment, all mice were sacrificed (cervical dislocation) and their livers and kidneys were removed; at the same time, the connective tissue on these organs was removed and washed with normal saline to remove blood.

2.6.2. Biochemical Analysis

Blood samples were centrifuged (4000 rpm, 4 °C, 20 min) and the supernatant was taken for analysis of NO, ET-1, urea, uric acid, and serum creatinine content using an automatic serum biochemical analyzer (BS-240VET, Beijing, China) according to the manufacturer's instructions.

2.6.3. Organ Cadmium Content Analysis

Taking appropriate serum, heart, kidney, and liver samples, cadmium contents were analyzed using a diatomic fluorescence photometer (AFS-920, Beijing, China) [30].

2.6.4. Histopathological Analysis

Fresh liver samples were fixed in PBS buffer (pH 7.4) containing 10% formalin for over 24 h and embedded in paraffin. Thin sections (4–5 μm thickness) were prepared and stained with hematoxylin–eosin. These sections were viewed under a microscope (400× magnification) [31].

2.7. Statistical Analysis

All data were expressed as means ± standard deviations (M ± SD). Statistical analyses were performed by one-way ANOVA using the software program GraphPad Prizm 8.0. FTIR and TGA spectra were plotted using Origin 2019b. NMR spectra were analyzed using the software program MestreNova 14.0.

3. Results and Discussion

3.1. FTIR Analysis

The FTIR spectrum of ABPCP is shown in Figure 3. The intense and broad peak at 3371.34 cm^{-1} was due to hydroxyl groups with stretching vibration [32]. The peak at 2882.02 cm^{-1} was attributed to the C-H stretching vibration of the methyl group [33]. Absorption peaks were detected in the 1700–1300 cm^{-1} region, which indicated that the ABPCP had a carboxyl group, and the strong absorption at 1408.42 cm^{-1} was due to the C-H bending vibration. The peak at 1079.25 cm^{-1} confirmed the presence of a pyranose ring. The band at 897.73 cm^{-1} indicated the existence of a β-glycosidic bond [34].

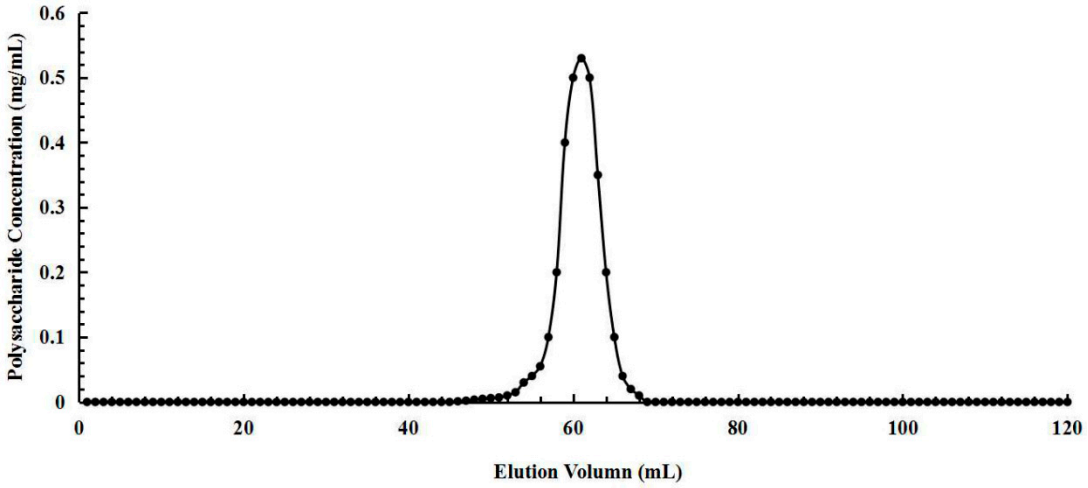


Figure 3. Purification of *Agaricus balchaschensis* polysaccharide (ABPCP) on DEAE-Sepharose chromatography and eluted with 0.5 M NaCl; flow rate 0.5 mL/min.

3.2. NMR Analysis

The solution-state HSQC NMR spectra of ABPCP were acquired, and are shown in Figure 4. In the HSQC spectrum, the δ_C/δ_H signal at 3.79/60.6 ppm corresponds to C6-H of (1 → 4)-linked α-D-glucan [35]. There were different Glc configurations in ABPCP: $^1H/^{13}C$ chemical shifts at δ_C/δ_H 3.39/75.5 and 3.62/60.7 ppm were assigned to H-5/C-5 H-6/C-6 of →3)-β-D-Glcp-(1 → residues [23]; and the cross-peaks (δ_C/δ_H 3.34/69.4, 3.75/75.1, and 3.57/80.5 ppm) were assigned to →3,6)-β-D-Glcp-(1→, →4)-β-D-GlcpA-(1→, and 4-*O*-Me-β-D-GlcpA-(1→, respectively [36–38]. The cross-peaks (δ_C/δ_H 4.09/68.8 and 3.74/68.8 ppm) were assigned to H-5/C-5 and H-6/C-6 of →6-β-D-Manp-(1→ residues, respectively [25]. δ_C/δ_H 3.64/75.8 ppm was assigned to H-3/C-3 of →6)-β-D-Galp-(1→ residues and δ_C/δ_H 4.65/102.2 ppm was associated with →3)-β-D-Galp-(1→ [36]. In addition, $^1H/^{13}C$ chemical shifts at δ_C/δ_H 4.41/102.8, 3.21/73.11, and 3.40/73.0 ppm

were assigned to C1-H, C2-H, and C3-H of (1 → 4)-linked β-D-xylan [33]. In summary, the polysaccharide in ABPCP was composed of α-glucan, (1 → 3)-linked β-D-Glcp, (1 → 4)-linked β-D-Glcp, (1 → 6)-linked β-D-Glcp, (1 → 6)-linked β-D-Manp, (1 → 3)-linked β-D-Galp, (1 → 6)-linked β-D-Galp, and (1 → 4)-linked β-D-xylan. This was consistent with the FTIR spectrum.

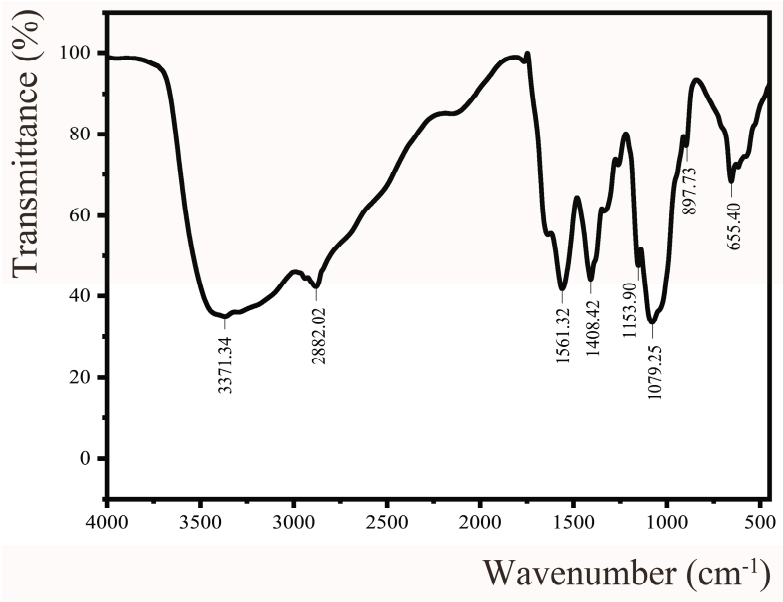


Figure 4. FTIR spectrum of ABPCP.

3.3. Thermogravimetric (TG) Analysis of ABPCP

Weight loss curves of ABPCP are shown in Figure 5. The TG curve showed two stages of weight loss. The first stage, resulting from the vaporization and removal of bound water in ABPCP, reflected the characteristic hygroscopicity based on the abundance of hydroxyl radicals. The second stage, which was due to the alteration of functional groups and the depolymerization of structure, resulted in a substantial loss of sample weight.

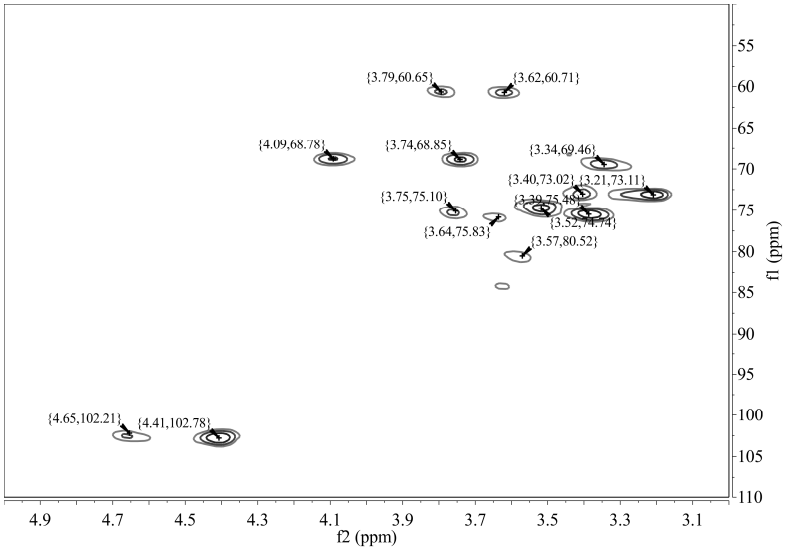


Figure 5. HSQC spectrum of ABPCP.

3.4. Amino Acid Composition Analysis

Kjeldahl nitrogen and circular dichroism were performed to verify the presence of peptides in polysaccharides. It was determined that the nitrogen content in the sample

was 891 mg/kg. This indicated the presence of nitrogen in the sample. The protein had been removed, so the substance containing nitrogen was the peptide. The results of CD and amino acid composition are shown in Figure 6 and Table 1. The amino acid content of ABPCP was 11.747 mg/g, and the content of Glu was the highest (Figure 7).

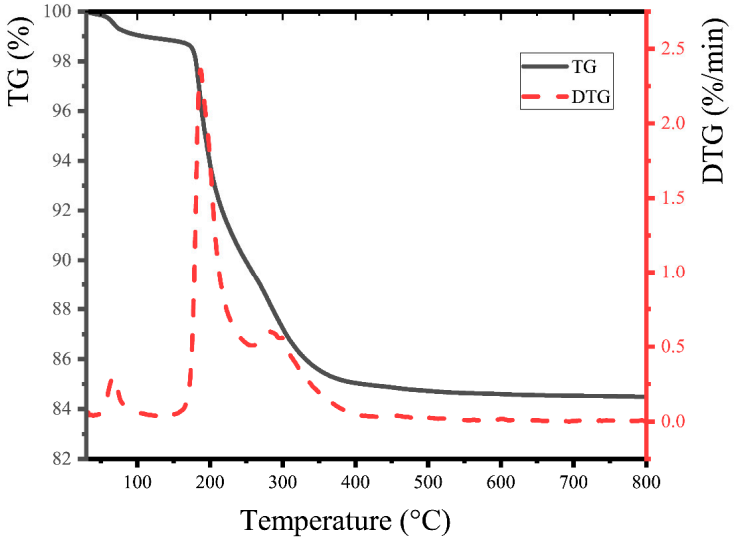


Figure 6. Weight loss (TG) percentage and derivative thermogravimetric (DTG) curves of ABPCP.

Table 1. The amino acid composition of ABPCP.

Amino Acid	Content (mg/g)
Asp	0.709
Thr	0.855
Ser	0.560
Glu	1.182
Gly	0.757
Ala	0.383
Cys	4.898
Val	0.926
Met	0.279
Lys	0.488
Arg	0.710

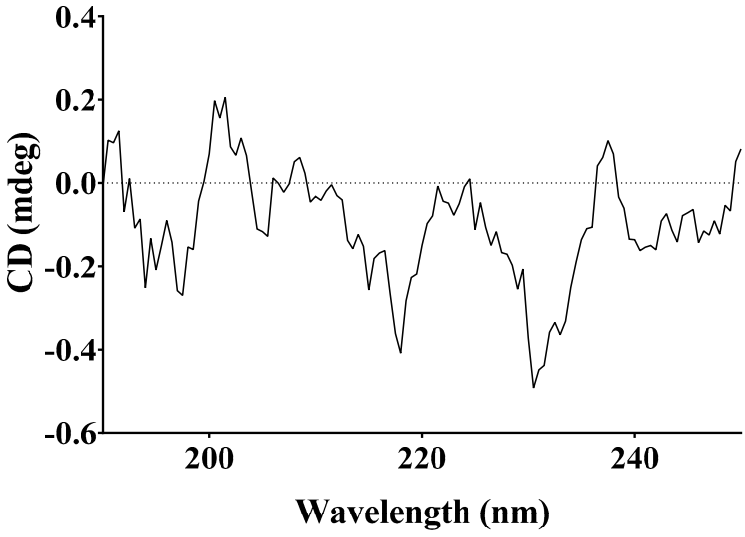


Figure 7. CD spectra of ABPCP.

3.5. The Ability of ABPCP to Reduce Heavy Metals Toxicity In Vivo

In this study, biochemical analysis, organ cadmium content analysis, and histopathological observation of the heart, kidneys, liver, and serum samples were conducted to validate the ability of ABPCP to alleviate cadmium toxicity. Exposure to cadmium-induced liver and kidney damage elevated the levels of serum urea, uric acid, creatinine, nitric oxide, and endothelin in mice. As shown in Tables 2–6, after administration of ABPCP, the contents of uric acid, urea, creatinine, endothelin, and nitric oxide in the serum significantly decreased, presenting a dose-dependent effect. After gavage of 100 mg/kg ABPCP, the serum uric acid content, urea content, serum creatinine content, endothelin-1 content, and nitric oxide content were reduced several times compared with those of the NG, with values approaching the normal range. As shown in Table 7, exposure to cadmium resulted in cadmium accumulation in the serum, heart, kidneys, and liver. Nevertheless, gavaging with ABPCP decreased the cadmium content in the serum, heart, kidneys, and liver. Intragastric administration of ABPCP significantly reduced the cadmium content in the serum, heart, kidneys, and liver. After ABPCP treatment, the cadmium content in the heart, kidneys, and serum of mice was reduced by approximately three times, and the cadmium content in the liver was reduced by approximately two to three times.

Table 2. Changes in uric acid content in serum.

Group	7 d	14 d	21 d
CK	1.63 ± 0.29 C	1.18 ± 0.14 C	1.39 ± 0.08 C
NG	25.43 ± 1.76 A	25.26 ± 4.54 A	44.26 ± 3.28 A
DG-25	8.13 ± 1.74 B	7.86 ± 0.70 B	10.74 ± 0.21 B
DG-50	3.48 ± 0.58 C	2.24 ± 0.24 C	10.49 ± 0.05 B
DG-100	2.28 ± 0.06 C	1.96 ± 0.03 C	9.47 ± 0.49 B

Data are presented as mean ± standard deviation (n = 5). Different letters (A–C) indicate significant differences ($p < 0.01$). CK: vehicle control, normal saline. NG: negative control group, normal saline. DG-25: 25 mg/kg ABPCP, DG-50: 50 mg/kg ABPCP, DG-100: 100 mg/kg.

Table 3. Changes in urea content in serum.

Group	7 d	14 d	21 d
CK	10.3 ± 1.25 D	47.18 ± 5.98 D	44.58 ± 3.51 F
NG	313.83 ± 21.83 A	400.17 ± 29.16 A	370.7 ± 5.25 A
DG-25	95.91 ± 3.9 C	150.4 ± 6.6 B	190.9 ± 11.39 B
DG-50	35.9 ± 4.68 C	113.24 ± 5.35 C	168.17 ± 1.1 C
DG-100	5.6 ± 0.35 D	70.83 ± 3.55 D	91.5 ± 2.66 E

Data are presented as mean ± standard deviation (n = 5). Different letters (A–F) indicate significant differences ($p < 0.01$). CK: vehicle control, normal saline. NG: negative control group, normal saline. DG-25: 25 mg/kg ABPCP, DG-50: 50 mg/kg ABPCP, DG-100: 100 mg/kg.

Table 4. Changes in serum creatinine content in serum.

Group	7 d	14 d	21 d
CK	3.89 ± 0.39 D	1.98 ± 0.39 E	10.83 ± 0.60 CD
NG	47.71 ± 2.70 A	37.49 ± 3.9 A	44.30 ± 4.34 A
DG-25	23.67 ± 2.31 B	19.67 ± 1.26	22.53 ± 1.06 B
DG-50	16.4 ± 2.65 C	14.13 ± 3.53 BC	15.5 ± 1.57 C
DG-100	5.6 ± 0.35 D	5.83 ± 0.47 DE	7.98 ± 0.11 D

Data are presented as mean ± standard deviation (n = 5). Different letters (A–E) indicate significant differences ($p < 0.01$). CK: vehicle control, normal saline. NG: negative control group, normal saline. DG-25: 25 mg/kg ABPCP, DG-50: 50 mg/kg ABPCP, DG-100: 100 mg/kg.

Table 5. Changes in nitric oxide content in serum.

Group	7 d	14 d	21 d
CK	137.87 ± 1.56 E	134.80 ± 5.01 E	31.36 ± 12.29 E
NG	469.58 ± 12.12 A	413.47 ± 11.40 A	399.29 ± 6.46 A
DG-25	331.95 ± 8.90 B	276.91 ± 4.28 B	252.94 ± 5.03 B
DG-50	261.83 ± 3.60 C	209.76 ± 3.23 C	200.18 ± 4.38 C
DG-100	211.57 ± 2.98 D	177.6 ± 2.76 D	171.39 ± 3.69 D

Data are presented as mean ± standard deviation (n = 5). Different letters (A–E indicate significant differences ($p < 0.01$). CK: vehicle control, normal saline. NG: negative control group, normal saline. DG-25: 25 mg/kg ABPCP, DG-50: 50 mg/kg ABPCP, DG-100: 100 mg/kg.

Table 6. Changes in endothelin-1 content in serum.

Group	7 d	14 d	21 d
CK	29.38 ± 3.5 E	28.85 ± 3.58 E	142.90 ± 7.17 B
NG	286.19 ± 8.05 A	216.45 ± 9.29 A	178.89 ± 9.29 A
DG-50	133.29 ± 8.05 C	119.88 ± 4.65 C	93.06 ± 8.05 D
DG-25	189.62 ± 8.05 B	162.8 ± 12.29 B	141.34 ± 8.05 C
DG-100	109.15 ± 8.04 D	93.06 ± 8.05 D	60.87 ± 8.05 E

Data are presented as mean ± standard deviation (n = 5). Different letters (A–E) indicate significant differences ($p < 0.01$). CK: vehicle control, normal saline. NG: negative control group, normal saline. DG-25: 25 mg/kg ABPCP, DG-50: 50 mg/kg ABPCP, DG-100: 100 mg/kg.

Table 7. Content of cadmium in different organs.

Group	HEART	KIDNEY	LIVER	SERUM
CK	0.0044 ± 0.0023 D	0.03 ± 0.0054 C	0.02 ± 0.0012 D	0.00425 ± 0.0014 E
NG	2.83 ± 0.12 A	44.43 ± 4.54 A	91.28 ± 10.64 A	0.443 ± 0.058 A
DG-100	0.72 ± 0.040 C	13.27 ± 0.32 B	45.79 ± 1.43 B	0.129 ± 0.0053 D
DG-50	0.92 ± 0.022 B	15.23 ± 0.64 B	40.60 ± 1.21 BC	0.144 ± 0.015 CD
DG-25	0.95 ± 0.076 B	16.97 ± 0.50 B	31.24 ± 2.49 C	0.1925 ± 0.013 BC

Data are presented as mean ± standard deviation (n = 5). Different letters (A–E) indicate significant differences ($p < 0.01$). CK: vehicle control, normal saline. NG: negative control group, normal saline. DG-25: 25 mg/kg ABPCP, DG-50: 50 mg/kg ABPCP, DG-100: 100 mg/kg.

As shown in Figure 6, extensive kidney damage in Cd^{2+}-treated mice was observed compared to the normal group. There was destruction at the glomerulus, tubulointerstitial lesions, and glomerular interstitial expansion in the Cd^{2+}-treated group. Although there were still pathological changes, including inflammatory cell infiltration and congestion in the ABPCP-treated groups, it was significant that ABPCP reduced glomerular interstitial expansion. The damage to the liver was minor, but the effect was similar. In comparison with a normal liver, cellular degeneration, hepatocyte necrosis, and lipid droplet accumulation were observed in Cd^{2+}-treated mice. Feeding with ABPCP ameliorated kidney and liver damage by the diminution of necrotic zones and color change. The medium and high doses were better.

It is well known that the kidneys and liver are the main target organs for heavy metals accumulation and toxicity [39]. Heavy metals induce oxidative stress by generating free radicals and reducing antioxidant levels [40], which is one of the primary mechanisms of heavy metal-induced injury. Two polysaccharides from *Panax notoginseng* with →3)-D-Glcp-(1→, →3, 6)-D-Glcp-(1→ and →3)-β-Galp-(1→ residues, which was also detected in ABPCP, displayed antioxidant activity in vivo [40], and these residues may be associated with antioxidant activity. This indicated that ABPCP alleviated kidney and liver injury through antioxidant activity.

Cadmium is a highly toxic heavy metal element that can enter the body through air, food, and other means and accumulate in organs such as the kidneys, liver, heart, and

lungs, causing irreversible damage to them [41]. Cadmium can cause damage to the liver and kidneys and lead to an increase in serum levels of uric acid, urea, creatinine, and nitric oxide [42]. In our study, ABPCP significantly reduced serum urea, uric acid, creatinine, nitric oxide, and endothelin-1 in cadmium-damaged mice, alleviated glomerular interstitial expansion, and reduced liver and kidney tissue necrosis. These results suggest that ABPCP can alleviate cadmium-induced liver and kidney damage.

Polysaccharides exhibit numerous activities, such as antioxidant, hypoglycemic, and anti-inflammatory activities, and metal ion chelation [43]. The binding ability of heavy metal ions is affected by the structure of the polysaccharide [44]. In this study, a peptide-containing polysaccharide was isolated from *A. balchaschensis* to alleviate cadmium-induced kidney and liver damage. Studies have found that ABPCP can significantly reduce the cadmium content in the serum, heart, kidneys, and liver of mice. We hypothesized that ABPCP can reduce the cadmium content because the peptide chain contains carboxyl groups, which can bind with chromium ions, thereby reducing the absorption of cadmium in mice and consequently reducing the accumulation of cadmium in mice. Therefore, these results indicated that ABPCP could reduce cadmium accumulation in organs and mitigate the damage caused by cadmium (Figures 8 and 9).

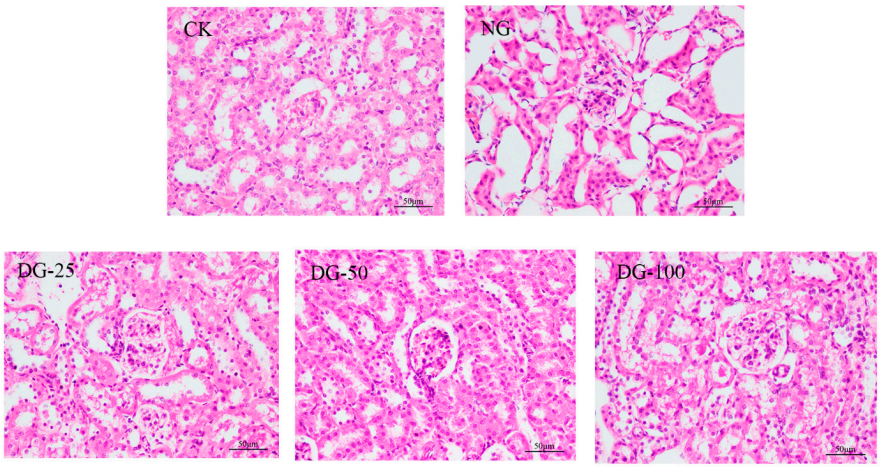


Figure 8. Effect of ABPCP on morphological changes in kidneys from Cd-induced mice (hematoxylin–eosin staining, magnification 400×).

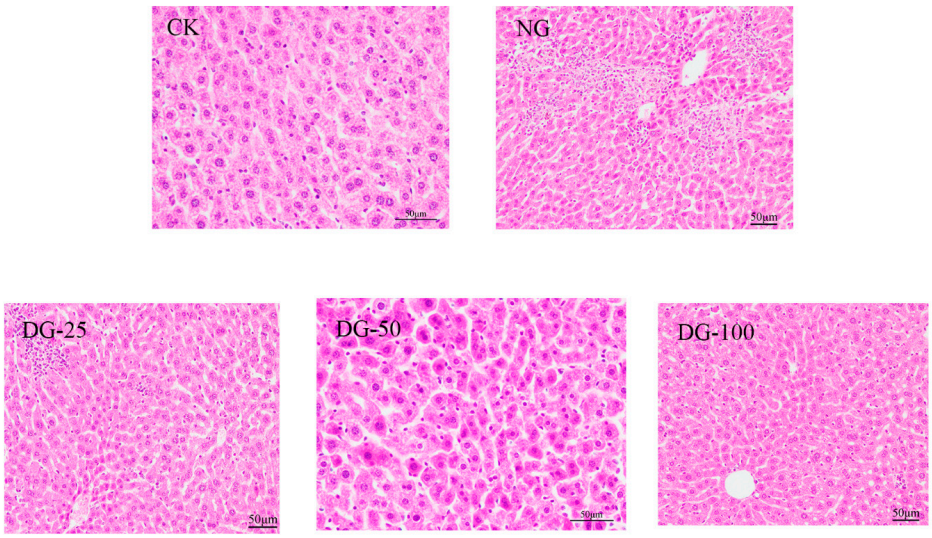


Figure 9. Effect of ABPCP on morphological changes in livers from Cd-induced mice (hematoxylin–eosin staining, magnification 400×).

4. Conclusions

In this study, a lesser known peptide-containing polysaccharide was extracted using a pioneering method. We focused on the structural analysis of ABPCP, which confirmed that it was a substance with peptides attached to a polysaccharide chain. ABPCP can alleviate cadmium injury by reducing the cadmium content in the serum, heart, kidneys, and liver and reduce serum urea, uric acid, serum creatinine, nitric oxide, and endothelin-1 in cadmium-damaged mice. Therefore, our research on ABPCP may provide new insight into the application of polysaccharide–peptide conjugates.

Author Contributions: These experiments were jointly designed and conceptualized by N.Y., Y.D., X.F. and J.H., with the project being executed by N.Y., C.L. and Y.D. as the principal investigator. Experimental data were analyzed by Y.L. and P.J. Animal experiments were conducted by N.Y., Z.L. and H.C.; W.J. and Q.Z. collected the basidiocarps of *A. balchaschensis*. N.Y., X.F. and J.H. participating in writing academic papers. All authors have read and agreed to the published version of the manuscript.

Funding: This study was supported by a grant from the National Natural Science Foundation of China (grant number: 32060709) and was a special project for basic scientific activities of non-profit institutes supported by the government of the Xinjiang Uyghur Autonomous Region (grant number: KY2022044).

Data Availability Statement: Data are contained within the article.

Conflicts of Interest: The authors declare that they have no known competing financial interest or personal relationships that could influence the study described in this article.

References

1. Huang, Y.; Ye, Y.; Xu, D.; Ji, J.; Sun, J.; Xu, M.; Xia, B.; Shen, H.; Xia, R.; Shi, W.; et al. Structural characterization and anti-inflammatory activity of a novel neutral polysaccharide isolated from *Smilax glabra* Roxb. *Int. J. Biol. Macromol.* **2023**, *234*, 123559. [CrossRef] [PubMed]
2. Zhu, Z.-P.; Lin, W.; Ma, J.-X.; Li, N.; Wang, J.-X.; Li, J.-M. The physiochemical characteristics of *Cyclocarya paliurus* polysaccharides and in vitro anti-diabetic effects of their different fractions. *Ind. Crops Prod.* **2024**, *211*, 118188. [CrossRef]
3. Chen, S.K.; Wang, X.; Guo, Y.Q.; Song, X.X.; Yin, J.Y.; Nie, S.P. Exploring the partial degradation of polysaccharides: Structure, mechanism, bioactivities, and perspectives. *Compr. Rev. Food. Sci. Food Saf.* **2023**, *22*, 4831–4870. [CrossRef] [PubMed]
4. Taghizadeh, M.S.; Taherishirazi, M.; Niazi, A.; Afsharifar, A.; Moghadam, A. Structure guided design and cloning of peptide inhibitors targeting CDK9/cyclin T1 protein protein interaction. *Front. Pharmacol.* **2024**, *15*, 1327820. [CrossRef] [PubMed]
5. Taghizadeh, M.S.; Niazi, A.; Mirzapour-Kouhdasht, A.; Pereira, E.C.; Garcia-Vaquero, M. Enhancing cyclotide bioproduction: Harnessing biological synthesis methods and various expression systems for large-scale manufacturing. *Crit. Rev. Biotechnol.* **2024**, *7*, 1–23. [CrossRef]
6. Olech, M.; Cybulska, J.; Nowacka-Jechalke, N.; Szpakowska, N.; Maslyk, M.; Kubinski, K.; Martyna, A.; Zdunek, A.; Kaczynski, Z. Novel polysaccharide and polysaccharide-peptide conjugate from *Rosa rugosa* Thunb. pseudofruit-Structural characterisation and nutraceutical potential. *Food Chem.* **2023**, *409*, 135264. [CrossRef] [PubMed]
7. Lv, X.-C.; Guo, W.-L.; Li, L.; Yu, X.-D.; Liu, B. Polysaccharide peptides from *Ganoderma lucidum* ameliorate lipid metabolic disorders and gut microbiota dysbiosis in high-fat diet-fed rats. *J. Funct. Foods* **2019**, *57*, 48–58. [CrossRef]
8. Fang, H.; Li, X.; Lin, D.; Wang, L.; Yang, T.; Yang, B. Inhibition of intrarenal PRR-RAS pathway by *Ganoderma lucidum* polysaccharide peptides in proteinuric nephropathy. *Int. J. Biol. Macromol.* **2023**, *253*, 127336. [CrossRef]
9. Meng, M.; Wang, L.; Yao, Y.; Lin, D.; Wang, C.; Yao, J.; Sun, H.; Liu, M. *Ganoderma lucidum* polysaccharide peptide (GLPP) attenuates rheumatic arthritis in rats through inactivating NF-kappaB and MAPK signaling pathways. *Phytomedicine* **2023**, *119*, 155010. [CrossRef]
10. Xie, J.; Lin, D.; Li, J.; Zhou, T.; Lin, S.; Lin, Z. Effects of *Ganoderma lucidum* polysaccharide peptide ameliorating cyclophosphamide-induced immune dysfunctions based on metabolomics analysis. *Front. Nutr.* **2023**, *10*, 1179749. [CrossRef] [PubMed]
11. Meng, J.; Ma, A.; Zhang, S.; Lin, D.; Lin, S.; Li, M.; Zhou, H.; Yang, B. *Ganoderma lucidum* Polysaccharide Peptide attenuates post myocardial infarction fibrosis via down-regulating TGF-β1/SMAD and relieving oxidative stress. *Pharmacol. Res.-Mod. Chin. Med.* **2022**, *4*, 100152. [CrossRef]

12. Nauroze, T.; Ali, S.; Kanwal, L.; Ara, C.; Akbar Mughal, T.; Andleeb, S. Ameliorative effect of *Nigella sativa* conjugated silver nanoparticles against chromium-induced hepatotoxicity and renal toxicity in mice. *Saudi J. Biol. Sci.* **2023**, *3*, 103571. [CrossRef]
13. Ghosh, P.; Dey, T.; Majumder, R.; Datta, M.; Chattopadhyay, A.; Bandyopadhyay, D. Insights into the antioxidative mechanisms of melatonin in ameliorating chromium-induced oxidative stress-mediated hepatic and renal tissue injuries in male Wistar rats. *Food Chem. Toxicol.* **2023**, *173*, 113630. [CrossRef]
14. Wongmekiat, O.; Peerapanyasut, W.; Kobroob, A. Catechin supplementation prevents kidney damage in rats repeatedly exposed to cadmium through mitochondrial protection. *Naunyn-Schmiedeberg's Arch Pharmacol.* **2018**, *391*, 385–394. [CrossRef] [PubMed]
15. Dastan, D.; Karimi, S.; Larki-Harchegani, A.; Nili-Ahmadabadi, A. Protective effects of *Allium hirtifolium* Boiss extract on cadmium-induced renal failure in rats. *Environ. Sci. Pollut. R.* **2019**, *26*, 18886–18892. [CrossRef] [PubMed]
16. Mohanty, S.; Benya, A.; Hota, S.; Kumar, M.S.; Singh, S. Eco-toxicity of hexavalent chromium and its adverse impact on environment and human health in Sukinda Valley of India: A review on pollution and prevention strategies. *Environ. Chem. Ecotoxicol.* **2023**, *5*, 46–54. [CrossRef]
17. Chen, Q.; Zhang, R.; Li, W.M.; Niu, Y.J.; Guo, H.C.; Liu, X.H.; Hou, Y.C.; Zhao, L.J. The protective effect of grape seed procyanidin extract against cadmium-induced renal oxidative damage in mice. *Environ. Toxicol. Pharmacol.* **2013**, *36*, 759–768. [CrossRef]
18. Varoni, M.V.; Pasciu, V.; Gadau, S.D.; Baralla, E.; Serra, E.; Palomba, D.; Demontis, M.P. Possible antioxidant effect of *Lycium barbarum* polysaccharides on hepatic cadmium-induced oxidative stress in rats. *Environ. Sci. Pollut. Res. Int.* **2017**, *24*, 2946–2955. [CrossRef]
19. Akinyemi, A.J.; Okonkwo, P.K.; Faboya, O.A.; Onikanni, S.A.; Fadaka, A.; Olayide, I.; Akinyemi, E.O.; Oboh, G. Curcumin improves episodic memory in cadmium induced memory impairment through inhibition of acetylcholinesterase and adenosine deaminase activities in a rat model. *Metab. Brain Dis.* **2017**, *32*, 87–95. [CrossRef]
20. Mizuno, M.; Minato, K.I. Anti-inflammatory and immunomodulatory properties of polysaccharides in mushrooms. *Curr. Opin. Biotechnol.* **2024**, *86*, 103076. [CrossRef] [PubMed]
21. Yu, Y.; Liu, Z.; Song, K.; Li, L.; Chen, M. Medicinal value of edible mushroom polysaccharides: A review. *J. Future Foods* **2023**, *3*, 16–23. [CrossRef]
22. Zhao, Q.; Jiang, Y.; Zhao, Q.; Patrick Manzi, H.; Su, L.; Liu, D.; Huang, X.; Long, D.; Tang, Z.; Zhang, Y. The benefits of edible mushroom polysaccharides for health and their influence on gut microbiota: A review. *Front. Nutr.* **2023**, *10*, 1213010. [CrossRef] [PubMed]
23. Muhaxi, M.; Liu, F.; Ng, T.B. Structural characterization and in vitro hepatoprotective activity of a novel antioxidant polysaccharide from fruiting bodies of the mushroom *Pleurotus ferulae*. *Int. J. Biol. Macromol.* **2023**, *243*, 125124. [CrossRef] [PubMed]
24. Tsai, C.H.; Yen, Y.H.; Yang, J.P. Finding of polysaccharide-peptide complexes in *Cordyceps militaris* and evaluation of its acetylcholinesterase inhibition activity. *J. Food Drug Anal.* **2015**, *23*, 63–70. [CrossRef] [PubMed]
25. Feng, X.; Wang, P.; Lu, Y.; Zhang, Z.; Yao, C.; Tian, G.; Liu, Q. A Novel Polysaccharide From *Heimioporus retisporus* Displays Hypoglycemic Activity in a Diabetic Mouse Model. *Front. Nutr.* **2022**, *9*, 964948. [CrossRef] [PubMed]
26. Chen, W.; Lu, Y.; Hu, D.; Mo, J.; Ni, J. Black mulberry (*Morus nigra* L.) polysaccharide ameliorates palmitate-induced lipotoxicity in hepatocytes by activating Nrf2 signaling pathway. *Int. J. Biol. Macromol.* **2021**, *172*, 394–407. [CrossRef]
27. Nguyen, T.A.; Do, T.T.; Nguyen, T.D.; Pham, L.D.; Nguyen, V.D. Isolation and characteristics of polysaccharide from *Amorphophallus corrugatus* in Vietnam. *Carbohyd. Polym.* **2011**, *84*, 64–68. [CrossRef]
28. Micsonai, A.; Wien, F.; Kernya, L.; Lee, Y.H.; Goto, Y.; Refregiers, M.; Kardos, J. Accurate secondary structure prediction and fold recognition for circular dichroism spectroscopy. *Proc. Natl. Acad. Sci. USA* **2015**, *112*, E3095–E3103. [CrossRef]
29. Fountoulakis, M.; Lahm, H.-W. Hydrolysis and amino acid composition analysis of proteins. *J. Chromatogr. A* **1998**, *826*, 109–134. [CrossRef] [PubMed]
30. Ma, Y.; Yue, C.; Sun, Q.; Wang, Y.; Gong, Z.; Zhang, K.; Da, J.; Zou, H.; Zhu, J.; Zhao, H.; et al. Cadmium exposure exacerbates kidney damage by inhibiting autophagy in diabetic rats. *Ecotoxicol. Environ. Saf.* **2023**, *186*, 144544. [CrossRef]
31. Guo, J.; Low, J.H.; Rajagopal Iyer, V.; Wong, P.; Ong, C.B.; Loh, W.L.; Yeow, C.H. A Preliminary Study on Grip-Induced Nerve Damage Caused by a Soft Pneumatic Elastomeric Gripper. *Polymers* **2022**, *14*, 4272. [CrossRef]
32. Oiu, J.; Shi, W.; Miao, J.; Hu, H.; Gao, Y. Extraction, Isolation, Screening, and Preliminary Characterization of Polysaccharides with Anti-Oxidant Activities from *Oudemansiella raphanipies*. *Polymers* **2023**, *15*, 2917. [CrossRef] [PubMed]
33. Wang, W.; Li, X.; Bao, X.; Gao, L.; Tao, Y. Extraction of polysaccharides from black mulberry fruit and their effect on enhancing antioxidant activity. *Int. J. Biol. Macromol.* **2018**, *120*, 1420–1429. [CrossRef] [PubMed]
34. Zhang, Y.; Zhou, T.; Wang, H.; Cui, Z.; Cheng, F.; Wang, K.P. Structural characterization and in vitro antitumor activity of an acidic polysaccharide from *Angelica sinensis* (Oliv.) Diels. *Carbohydr. Polym.* **2016**, *147*, 401–408. [CrossRef] [PubMed]
35. Li, M.-F.; Fan, Y.-M.; Xu, F.; Sun, R.-C. Structure and thermal stability of polysaccharide fractions extracted from the ultrasonic irradiated and cold alkali pretreated bamboo. *J. Appl. Polym. Sci.* **2011**, *121*, 176–185. [CrossRef]
36. Choi, J.W.; Synytsya, A.; Capek, P.; Bleha, R.; Pohl, R.; Park, Y.I. Structural analysis and anti-obesity effect of a pectic polysaccharide isolated from Korean mulberry fruit Oddi (*Morus alba* L.). *Carbohydr. Polym.* **2016**, *146*, 187–196. [CrossRef] [PubMed]

37. Kono, H.; Kondo, N.; Hirabayashi, K.; Ogata, M.; Totani, K.; Ikematsu, S.; Osada, M. NMR spectroscopic structural characterization of a water-soluble beta-(1→3, 1→6)-glucan from *Aureobasidium pullulans*. *Carbohydr. Polym.* **2017**, *174*, 876–886. [CrossRef]
38. Liu, X.; Liu, D.; Chen, Y.; Zhong, R.; Gao, L.; Yang, C.; Ai, C.; El-Seedi, H.R.; Zhao, C. Physicochemical characterization of a polysaccharide from *Agrocybe aegirita* and its anti-ageing activity. *Carbohydr. Polym.* **2020**, *236*, 116056. [CrossRef] [PubMed]
39. Fu, Z.; Xi, S. The effects of heavy metals on human metabolism. *Toxicol. Mech. Methods* **2020**, *30*, 167–176. [CrossRef]
40. Feng, S.; Cheng, H.; Xu, Z.; Feng, S.; Yuan, M.; Huang, Y.; Liao, J.; Ding, C. Antioxidant and anti-aging activities and structural elucidation of polysaccharides from *Panax notoginseng* root. *Process Bioch.* **2019**, *78*, 189–199. [CrossRef]
41. Ying, X.; Pan, Y.; Lan, J.; Fang, Y.; Ding, Y.; Gu, Z. Preparation of pectin from fingered citron peel and its protective effect on cadmium-induced liver and kidney damage in mice. *Food Biosci.* **2023**, *56*, 103359. [CrossRef]
42. Han, P.; Tian, X.; Wang, H.; Ju, Y.; Sheng, M.; Wang, Y.; Cheng, D. Purslane (*Portulacae oleracea* L.) polysaccharide relieves cadmium-induced colonic impairments by restricting Cd accumulation and inhibiting inflammatory responses. *Int. J. Biol. Macromol.* **2024**, *257*, 128500. [CrossRef] [PubMed]
43. Tian, X.; Ding, Y.; Kong, Y.; Wang, G.; Wang, S.; Cheng, D. Purslane (*Portulacae oleracea* L.) attenuates cadmium-induced hepatorenal and colonic damage in mice: Role of chelation, antioxidant and intestinal microecological regulation. *Phytomedicine* **2021**, *92*, 153716. [CrossRef] [PubMed]
44. Musarurwa, H.; Tawanda, T.N. Application of carboxymethyl polysaccharides as bio-sorbents for the sequestration of heavy metals in aquatic environments. *Carbohydr. Polym.* **2020**, *237*, 116142. [CrossRef] [PubMed]

Disclaimer/Publisher's Note: The statements, opinions and data contained in all publications are solely those of the individual author(s) and contributor(s) and not of MDPI and/or the editor(s). MDPI and/or the editor(s) disclaim responsibility for any injury to people or property resulting from any ideas, methods, instructions or products referred to in the content.